Proximal Federated Learning for Body Mass Index Monitoring using Commodity WiFi

Jiaxi Li
University of Georgia
Athens, Georgia, USA

Kiran Davuluri
Khairul Mottakin
Zheng Song
University of Michigan
Dearborn, Michigan, USA

Fei Dou
Jin Lu
University of Georgia
Athens, Georgia, USA

Abstract

Body Mass Index (BMI) is a critical metric for assessing public health and identifying populations at risk for obesity-related conditions. Traditional BMI monitoring methods often raise privacy concerns and require active cooperation from individuals, limiting their applicability in real-world scenarios. This paper introduces a novel approach to BMI monitoring that leverages proximal federated learning (PFL) using commodity WiFi devices. Our method addresses the challenges of data heterogeneity and intermittent connectivity in FL. By our approach, the Adaptive Elastic Stochastic Alternating Direction Method of Multipliers (AESADMM), an optimization algorithm designed to handle data heterogeneity and intermittent connectivity in FL scenarios, our system collects Channel State Information (CSI) from WiFi signals to passively classify BMI based on the impact of different body shapes on signal propagation. This approach ensures privacy preservation and eliminates the need for active participant involvement. Theoretical analysis and empirical results demonstrate the superior accuracy, reduced communication costs, and enhanced scalability of our proposed method compared to existing personalized FL frameworks, showcasing its potential as an effective tool for large-scale BMI monitoring in diverse environments.

Keywords

Channel State Information (CSI), WiFi Sensing, Federated Learning, BMI Classification

ACM Reference Format:
Jiaxi Li, Kiran Davuluri, Khairul Mottakin, Zheng Song, Fei Dou, and Jin Lu. 2024. Proximal Federated Learning for Body Mass Index Monitoring using Commodity WiFi. In *International Workshop on Physics Embedded AI Solutions in Mobile Computing (PICASSO 24), November 18–22, 2024, Washington D.C., DC, USA.* ACM, New York, NY, USA, 5 pages. https://doi.org/10.1145/3636534.3694735

1 Introduction

Body Mass Index (BMI), calculated from an individual's weight and height, is a vital indicator used to assess body fat and identify health risks associated with underweight and obesity [25]. Community-level BMI monitoring is essential for public health authorities to track prevalence and trends, evaluate intervention efficacy, and develop strategies to promote healthy weight and prevent related health issues [16]. However, traditional BMI monitoring methods often pose significant privacy concerns and require active cooperation from individuals, which limits their practicality and scalability.

Existing BMI monitoring approaches include obtaining patient records from healthcare systems [1], recruiting participants for self-reported measurements [3], and utilizing image processing techniques for BMI estimation [7, 8]. While these methods have their merits, they also present challenges such as privacy violations, resource-intensive processes, and limited long-term applicability. Therefore, there is an urgent need for a fine-grained, cost-effective, and privacy-preserving BMI monitoring solution that can be implemented over extended periods without compromising individual privacy.

In response to these challenges, this paper introduces a novel approach to BMI monitoring called proximal federated learning (PFL) in environments with inconsistent connectivity, utilizing commodity WiFi devices. Our methodology, the Adaptive Elastic Stochastic Alternating Direction Method of Multipliers (AESADMM), is an optimization algorithm tailored to address data heterogeneity and intermittent connectivity in federated learning scenarios. By passively collecting Channel State Information (CSI) from WiFi signals, our system classifies BMI by analyzing the impact of different body shapes on signal propagation, ensuring privacy preservation and obviating the need for active participant involvement. The key contributions of our work are as follows:

1. We present the novel proximal federated learning framework for BMI monitoring using commodity WiFi, addressing the challenges of data heterogeneity and intermittent connectivity [5].

2. We set up a WiFi sensing system using off-the-shelf devices to collect CSI. Using our system, we collected CSI data for 30 human subjects with varied BMI. Our approach leverages CSI to classify BMI in a privacy-preserving manner, providing a fine-grained, cost-effective solution suitable for large-scale deployment.

3. We demonstrate the theoretical and empirical effectiveness of our proposed method, achieving significant improvements in accuracy, reduced communication costs, and enhanced scalability compared to existing personalized FL frameworks.

The remainder of this paper is organized as follows: Section 2 provides a review of work in the related domain. Section 3 introduces our methodology, and Section 4 reports how we evaluated the effectiveness of our approach. Finally, we conclude this paper with Section 5.

PICASSO 24, November 18–22, 2024, Washington D.C., DC, USA

ACM ISBN 979-8-4007-0489-5/24/11
https://doi.org/10.1145/3636534.3694735

2 Related Works

2.1 Heterogeneous Federated Learning

Federated Learning (FL) represents a decentralized machine learning paradigm where multiple clients can collaboratively develop a global model without exchanging their local datasets. This methodology effectively mitigates privacy issues but encounters notable obstacles in infrastructure-deficient settings with varied data characteristics. Traditional FL strategies, such as Federated Averaging (FedAvg), are less effective with non-IID (non-independent and identically distributed) datasets, often resulting in compromised global model accuracy [14]. To address these limitations, recent innovations in personalized FL techniques have sought to tailor models more closely to the unique data distributions of individual clients [10, 11, 21, 22]. Nonetheless, these approaches typically presume the availability of consistent connectivity and a central coordination mechanism, which may not be feasible in many practical contexts. An emergent technique, the Random Walk Stochastic Alternating Direction Method of Multipliers (RWSADMM) utilizes a mobile server that dynamically moves among clients. Such a design is particularly effective in environments with sporadic connectivity and heterogeneous data, enhancing robustness [17]. However, RWSADMM's requirement to mobilize servers under such conditions renders it difficult for applications like Body Mass Index (BMI) monitoring through WiFi sensing.

2.2 Channel State Information (CSI)

Fine-grained Channel State Information (CSI) is extensively utilized to delineate the behavior of WiFi signals as they encounter various obstructions, as noted by Zhou et al. [30]. All WiFi protocols employ Orthogonal Frequency-Division Multiplexing (OFDM), which allocates the available spectrum across multiple sub-carriers [27]. Unlike the Received Signal Strength Indicator (RSSI), which provides a singular measure of signal strength by averaging across sub-carriers, CSI offers detailed insights at the level of each sub-carrier, thus enabling more granular analysis. The CSI can be represented as a three-dimensional tensor corresponding to t transmitting and r receiving antennas:

$$CSI = \begin{bmatrix} H_{1,1} & \dots & H_{1,r} \\ \vdots & \ddots & \vdots \\ H_{t,1} & \dots & H_{t,r} \end{bmatrix} \tag{1}$$

Here, $H_{t,r}$ denotes a vector containing complex pairs for each sub-carrier, as shown in Eq. (2).

$$H_{t,r} = [h_{t,r,1}, \dots, h_{t,r,m}] \tag{2}$$

The variable m indicates the number of data sub-carriers, where each $H_{t,r}$ is expressed as a complex number h_m, encapsulating both the amplitude ($|h_m|$) and phase ($\angle h_m$) of CSI. The values of amplitude and phase are susceptible to alterations caused by multipath effects, such as phase shifts and amplitude attenuation, which are exacerbated by human movements. This sensitivity to changes makes CSI a powerful tool for precisely sensing and locating human subjects, as demonstrated by Xin et al. [26].

2.3 BMI Classification

Body Mass Index (BMI) is calculated by assessing an individual's body fat based on their weight and height using the formula: $\text{BMI} = \frac{\text{Weight (lb)}}{[\text{Height (in)}]^2} \times 703$. This metric is crucial for evaluating health risk factors. Adults are typically categorized into one of four BMI classifications: *Obese*, *Overweight*, *Normal Weight*, and *Underweight*. Figure 1 illustrates the impact of weight and height on BMI categorization.

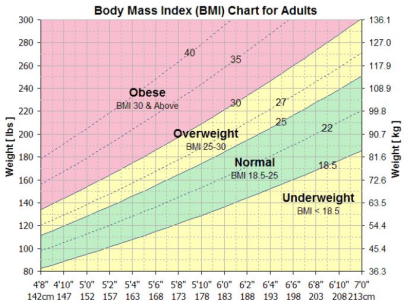

Figure 1: BMI Chart for Adults

Section 1 reviews various techniques for monitoring BMI. Recently, the focus has shifted towards the use of computer vision for BMI estimation, which offers a non-intrusive approach free from the need for participant engagement or access to medical records. This technology holds the promise of being seamlessly integrated into daily environments, enhancing both convenience and accessibility. Despite these advantages, machine learning-based BMI assessment raises significant privacy concerns, which are discussed in detail by Kumar et al. [9].

2.4 WiFi Sensing

Studies on bio-electromagnetism tailored to WiFi frequencies (such as 2.4 GHz and 5 GHz) have demonstrated that specific traits or gestures can be effectively detected when electromagnetic waves propagate at these particular frequencies [6]. This finding is fundamental to the development of WiFi-based sensing technologies. Over the past decade, numerous advancements have emerged [12], utilizing wireless communication channels to create innovative applications across human-computer interaction [19], healthcare monitoring [24], and security surveillance [29].

Inspired by the concept of unique pattern generation for active motion in the sensing region [15], body characterization research focuses on pose, person, gait, and activity recognition using statistical features extracted from CSI sequences [2, 13, 23]. Deep learning (DL) methods have been explored to enhance feature extraction from CSI data, thereby enhancing the robustness of CSI-based body characterization [27, 28]. Challenges such as overfitting and limited datasets persist, requiring dedicated layers for specific datasets. DL has shown success in sensorless body characterization and human activity recognition by applying transformation methods, with applications ranging from activity detection frameworks to small-scale recognition systems that address signal variations caused by movement speeds and body shapes [18].

3 Methodology

3.1 Overview

Figure 2 provides a comprehensive depiction of our model training structure, highlighting the mechanisms involved in gathering and analyzing Channel State Information (CSI) for BMI prediction in real-world environments and proximal federated learning scheme. To create a system suitable for practical deployment, we amassed a

substantial dataset from participants involved in a variety of experiments. This dataset includes a wide spectrum of individual body types, movement speeds, and motions such as rotating, walking backwards, and sidestepping, thereby enhancing the system's accuracy and reliability in real-world BMI assessment. For the purpose of BMI categorization, we converted the numerical CSI data into heatmaps depicted as 2D images. These are laid out on a two-dimensional plane with varying color intensities indicating different data values. These heatmaps are then used as inputs to train both conventional and cutting-edge machine learning models.

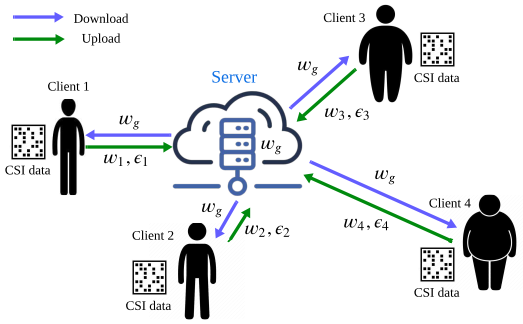

Figure 2: General Training Flow of Proximal Federated Learning. In each training round, global model w_g is downloaded from the server when the client is within the environment, the local model w_i and the proximity parameter ε_i are updated accordingly using local CSI data and uploaded to the server. Then the server update the global model.

3.2 Data Collection

For our experimental framework, we chose the Raspberry Pi (RPi), a widely accessible and cost-effective commodity device.

Thirty participants were randomly selected from the CIS department at UMDearborn. We gathered their body weights and heights to compute their Body Mass Indices (BMIs) and documented each participant's gender and age. Further details on our participants are available in Table 2.

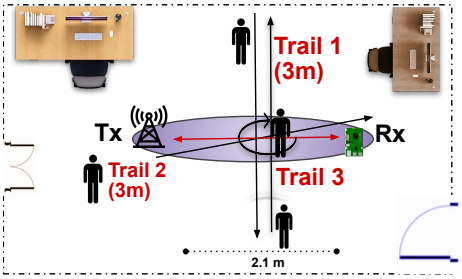

Figure 3: CSI Collection System Setup

Participants were instructed to walk along pre-defined trails in a 6m x 6m indoor lab room, with CSI samples recorded during their movement as illustrated in Fig. 3. The initial two trials consisted of walking at speeds ranging from 0.3 to 0.8 m/s across 3m-long paths, collecting 25 and 10 samples respectively. The third trial required participants to rotate 90 degrees every 2 seconds at the center of the Line of Sight (LoS), repeated five times.

System Settings	
Tx-Rx Height	0.5m
Tx-Rx Distance	2.1m
# of Subjects	30
Subject Movements/ Activity	Walking, Rotation
# of Trails	3
Sampling Duration	4-8 sec
Sampling Rate	200 Hz
CSI Samples	1050
Channel Frequency	80 MHz

Table 1: System Configuration

The setup was centrally placed in the room, with a Raspberry Pi (RPi) acting as a passive observer (Rx) measuring the CSI of WiFi signals emitted by an Access Point (Tx) approximately 2m away. A computer linked to the router stimulated traffic by sending 8000 ping packets to the Tx, while the RPi, in monitor mode, captured the return data. The number of packets was tailored to the duration of the activity. The sampling rate was maintained at 200 Hz to accurately capture participant movements. Data was collected using Nexmon, and processed with *tcpdump* to produce .pcap files. These files were then analyzed using CSIKit to generate 256 x 1 numpy matrices, which were further utilized in *Tensorflow* for extracting CSI amplitude data. This amplitude data was segmented using a sliding window of 1 second at 100Hz, with overlapping windows of 1 second. The configuration of our data collection system is summarized in Table 1.

BMI Category	Class Distribution (out of 1)	Age Range (in yrs)	Gender Ratio (Male:Female)	Weight Range (in kg)	Height Range (in m)
Underweight	0.133	19-25	4:0	50.4-57.0	1.67-1.78
Normal	0.6	23-40	13:5	53.8-75.5	1.63-1.86
Overweight	0.133	19-40	3:1	69.3-87.4	1.57-1.69
Obese	0.133	30-50	4:0	87.7-119.9	1.62-1.81

Table 2: Participant Distribution

3.3 Data Processing

The heatmaps depicted in Fig.4 were created using CSIKit[4], showcasing pseudo color maps that visualize signal variations over time, sub-carriers, and amplitude through RGB color intensities. The x-axis delineates time, the y-axis represents sub-carriers, and the z-axis (color intensity) indicates CSI amplitude levels. To reduce noise and maintain the integrity of the waveform in the CSI data collected via the Raspberry Pi, a Least-square smoothing filter [20] was employed with a sample window of 51 units.

3.4 Proximal Federated Learning for BMI Classification

Before we explore the specifics of the proposed algorithm, let's clarify the key notations. $\mathbf{x} \in \mathbb{R}^d$ represents a vector with length d and $\mathbf{e}$ is defined as a vector with entries equal to 1 and $\mathbf{X} \in \mathbb{R}^{l \times d}$ depicts a matrix with l rows and d columns. The inner product of A and B is shown as $\langle A, B \rangle$. $\odot$ represents the Hadamard product/element-wise product and $\otimes$ represents the Kronecker product between two matrices. Finally, Norm p of vector $\mathbf{x}$ is denoted as $||\mathbf{x}||_p^p = \sum_{i=1}^{d} |x_i|^p$, $\mathbf{x} \in \mathbb{R}^d$ and Frobenius norm of matrix $\mathbf{X}$ is written as $\|\mathbf{X}\|_F = \sqrt{\sum_{i=1}^{n} \sum_{j=1}^{m} |x_{ij}|^2}$.

Let's define the optimization problem for proximal Federated Learning (FL). Proximal FL can be modeled as an optimization problem on a connected graph $\mathcal{G} = (\mathcal{V}, \mathcal{E})$where we aim to learn a model collaboratively among n proximal clients. These clients

are represented as the vertex set $\mathcal{V} = v_1, v_2, \ldots, v_n, v_{glb}$, with v_{glb} denoting a global server node. The edge set $\mathcal{E}$.consists of n edges, each connecting a client v_i (where $i \in \{1, \ldots, n\}$, to the server v_{glb}. The weight of each edge corresponds to the disparity or distance between the model parameters at the two connected nodes. The goal of proximal FL is to minimize the collective loss function across all client nodes, subject to inequality constraints that maintain model proximity locally. Mathematically, the optimization problem is formulated as follows:

$$\min_{\mathbf{w}_{1:n} \in \mathbb{R}^p} \frac{1}{n} \sum_{i=1}^{n} [f_i(\mathbf{w}_i) + f_i(\mathbf{w}_{glb})] + \lambda \sum_{i=1}^{n} \varepsilon_i^2 \quad s.t. \ \|\mathbf{w}_i - \mathbf{w}_{glb}\| \leq \epsilon_i, \forall i \in \{1, \ldots, n\}. \tag{3}$$

where $f_i(\mathbf{w}_i)$ represents the local loss function with the model parameter as $\mathbf{w}_i$ for client i, and ε_i is the learnable proximal parameter. λ balances the trade-off between minimizing the expected loss and the proximity according to the differential distribution between clients and the global model. The proximal FL problem (3) can be expressed as:

$$\min_{\mathbf{w}_{glb}, \mathbf{W}} \ \frac{1}{n} F(\mathbf{W}, \mathbf{w}_{glb}) + \lambda \sum_{i=1}^{N} \varepsilon_i^2 \quad \text{s.t.} \ \ \|\mathbf{1} \otimes \mathbf{w}_{glb} - \mathbf{W}\|_2^2 \leq \mathbf{1} \otimes (\boldsymbol{\varepsilon}_1, ..., \boldsymbol{\varepsilon}_n)^2 / 2, \forall i. \tag{4}$$

where $\mathbf{1} = [1 \ 1 \ldots 1] \in \mathbb{R}^n$. We can obtain the augmented Lagrangian for problem (4)

$$L_\beta(\mathbf{w}_{glb}, \mathbf{W}, \mathbf{Z}_{1:n}) = \frac{1}{n}\Big[F(\mathbf{w}) + \sum_{i=1}^{n} < \mathbf{Z}_i, \|\mathbf{1} \otimes \mathbf{w}_{glb} - \mathbf{W}\|_2^2 - \boldsymbol{\varepsilon}_i^2 > + \frac{\beta}{2} \sum_{i=1}^{n} \|\|\mathbf{1} \otimes \mathbf{w}_{glb} - \mathbf{W}\|_2^2 - \varepsilon_i\|_F^2\Big]$$

where $\mathbf{Z}_i \in \mathbb{R}^{n_i p}$ are the dual variables and $\beta > 0$ is the barrier parameter. The Adaptive Elastic Stochastic Alternating Direction Method of Multipliers (AESADMM) algorithm minimizes the augmented Lagrangian $L_\beta(\mathbf{W}_{\text{glb}}, \mathbf{W}, \boldsymbol{\varepsilon}, \mathbf{Z}_{1:n})$ in an iterative manner. At each iteration k, only a subset of clients upload their model update to the server to participate in the federated update. The following updates are performed:

$$\arg\min_{\boldsymbol{\rho}_{i_k}} L_\beta(\mathbf{w}'_{glb}, \mathbf{w}'_{i_k}, \boldsymbol{\varepsilon}_{i_k}, \mathbf{z}'_{i_k}), \ \arg\min_{\mathbf{w}_{i_k}} L_\beta(\mathbf{w}'_{glb}, \mathbf{w}_{i_k}, \boldsymbol{\varepsilon}_{i_k}, \mathbf{z}'_{i_k}), \ \arg\min_{\mathbf{w}_{i_k}} L_\beta(\mathbf{w}_{glb}, \mathbf{W}, \boldsymbol{\varepsilon}_{i_k}, \mathbf{Z}'),$$

where $\mathbf{w}'_{glb}$, $\mathbf{w}_{i_k}$, and $\mathbf{z}'_{i_k}$ denote the groups of variables of the local parameters stored by client i_k at the $(k-1)$-th update.

Next, we derive the solver of each subproblem. The three steps are noted as Updating $\mathbf{w}_{i_k}$, Updating $\mathbf{w}_{glb}$, and Updating $\mathbf{z}_{i_k}$.

Updating $\mathbf{w}_{i_k}$:

$$\min_{\mathbf{w}_{i_k}} f_{i_k}(\mathbf{w}_{i_k}) + < \mathbf{z}'_{i_k}, \Big|\mathbf{w}'_{glb} - \mathbf{x}_{i_k}\Big| - \boldsymbol{\varepsilon}_{i_k} > + \frac{\beta}{2} \Big\|\Big|\mathbf{w}'_{glb} - \mathbf{x}_{i_k}\Big| - \boldsymbol{\varepsilon}_{i_k}\Big\|_2^2 > \tag{5}$$

The problem (5) can be solved iteratively, which may consume significant computational resources at the local clients. As the size of the local dataset increases, the computational complexity also escalates. By leveraging stochastic methods and first-order subgradient expansions, we derive a more computationally efficient approximation of the original problem as presented in Eq. (6):

$$\min_{\mathbf{w}_{i_k}} \Big[g_{i_k}(\mathbf{w}'_{i_k}, \boldsymbol{\xi}_{i_k})(\mathbf{w}_{i_k} - \mathbf{w}'_{i_k}) + < \mathbf{z}'_{i_k}, \Big|\mathbf{w}'_{glb} - \mathbf{w}_{i_k}\Big| - \boldsymbol{\varepsilon}_{i_k} > + \frac{\beta}{2} \Big\|\Big|\mathbf{w}'_{glb} - \mathbf{w}_{i_k}\Big| - \boldsymbol{\varepsilon}_{i_k}\Big\|_2^2 > \tag{6}$$

In Eq. (6), $\boldsymbol{\xi}_{i_k}$ denotes one or a few samples randomly selected by client i_k from its feature set and their ground truth labels in pairs at the k-th iteration. The function $g_{i_k}(\mathbf{w}'_{i_k}, \boldsymbol{\xi}_{i_k})$ is defined as the stochastic gradient of $f_{i_k}(\mathbf{w}'_{i_k})$ at $\mathbf{w}'_{i_k}$. The stochastic approximation can significantly reduce memory consumption and save computational costs in each iteration. By setting the subgradient of the objective function in Eq. (6) to zero, we can derive the closed-form solution in Eq. (7).

$$\begin{aligned} \mathbf{w}_{i_k} &= \mathbf{w}'_{glb} + \frac{1}{\beta}\mathbf{z}'_{i_k} \odot sgn(\mathbf{t}') - \frac{1}{\beta} sgn(\mathbf{t}') \odot (\boldsymbol{\varepsilon}_i + g_{i_k}(\mathbf{w}'_{i_k}, \boldsymbol{\xi}_{i_k})) \\ &= \mathbf{w}'_{glb} + \frac{1}{\beta} sgn(\mathbf{t}') \odot (\mathbf{z}'_{i_k} - \boldsymbol{\varepsilon}_i - g_{i_k}(\mathbf{w}'_{i_k}, \boldsymbol{\xi}_{i_k})) \end{aligned} \tag{7}$$

where the signum function $sgn(\cdot)$ extracts the signs of a vector and $\mathbf{t}'_{i_k} = \mathbf{w}'_{glb} - \mathbf{w}'_{i_k}$. Updating $\boldsymbol{\varepsilon}_i$ is similar to update $\mathbf{w}_{i_k}$.

Updating $\mathbf{w}_{glb}$: We solve the following problem

$$\min_{\mathbf{w}_{glb}} \langle \mathbf{Z}, \big|\mathbf{1} \otimes \mathbf{w}_{glb} - \mathbf{W}_{i_k}\big| - \mathbf{1} \otimes \boldsymbol{\varepsilon}_{i_k} \rangle + \frac{\beta}{2} \|\big|\mathbf{1} \otimes \mathbf{w}_{glb} - \mathbf{W}_{i_k}\big|\|_F - \mathbf{1} \otimes \boldsymbol{\varepsilon}_{i_k}^2 \tag{8}$$

One can readily derive a closed-form solution for the problem (8) as:

$$\mathbf{w}_{i_k} = \frac{1}{n_{i_k}} \sum_j \Big[\mathbf{w}_{i_k} - (\frac{\mathbf{z}_{i_k}}{\beta} + \boldsymbol{\varepsilon}_{i_k}) \odot sgn(\mathbf{t}_{i_k})\Big] \tag{9}$$

where $\mathbf{t}_{i_k} = \mathbf{w}'_{glb} - \mathbf{w}_{i_k}$ is similar to that of Eq. (7) except the updated $\mathbf{w}$. Specifically, via mathematical induction, we can attain the new updated form of $\mathbf{w}_{glb}$ below, which can also reduce the communication cost from $O(n)$ to $O(1)$.

$$\begin{aligned} \mathbf{w}_{glb} &= \mathbf{w}'_{glb} + \frac{1}{N}\Big[\mathbf{w}_{i_k} - (\frac{\mathbf{z}_{i_k}}{\beta} + \boldsymbol{\varepsilon}_{i_k}) \odot sgn(\mathbf{t}_{i_k})\Big] \\ &\quad - \Big[\mathbf{w}'_{i_k} - (\frac{\mathbf{z}'_{i_k}}{\beta} + \boldsymbol{\varepsilon}_{i_k}) \odot sgn(\mathbf{t}'_{i_k})\Big] \end{aligned} \tag{10}$$

Updating $\mathbf{z}_{i_k}$: The Lagrangian multiplier $\mathbf{z}_{i_k}$ can be updated strictly following the standard ADMM scheme below:

$$\mathbf{z}_{i_k} = \mathbf{z}'_{i_k} + \beta\Big[\mathbf{w}_{i_k} - \mathbf{w}'_{glb} - \boldsymbol{\varepsilon}_{i_k}\Big] \tag{11}$$

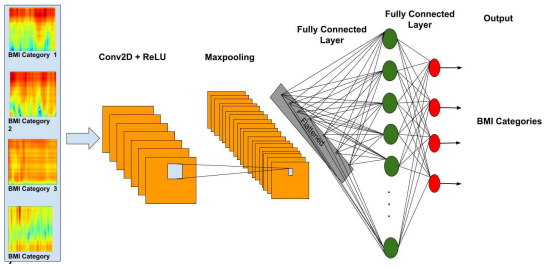

Figure 4: Training Neural Networks with Heatmaps

4 Evaluation

We collected a total of 1050 sampled 2D CSI images, and we randomly chose 900 samples for training and the remaining 150 for testing, as depicted in Table 3. In the training set, 20% of the samples were designated as the validation set. The training and test datasets underwent preprocessing steps including random resizing, cropping, horizontal flipping, and normalization. The models were initialized with pre-trained weights from ImageNet and had their last fully connected layer replaced with a linear layer tailored to the specific classification task. During training, each client's data was stored on a single edge device. The models were trained over 15 epochs, using a mini-batch size of 32 and updating parameters based on the cross-entropy loss function. Validation accuracy was calculated after each epoch to monitor performance on unseen data.

Metric /Model	ResNet-50			EffNet-B0		
	ARWSADMM	FedAVG	Local	ARWSADMM	FedAVG	Local
Train Accuracy	0.7410	0.6854	0.6625	0.5484	0.4484	0.4199
Validation Accuracy	0.6825	0.6237	0.5634	0.4243	0.4075	0.4021
Test F1 Score	0.7933	0.7306	0.7217	0.4942	0.3941	0.3901
Test Precision	0.7541	0.7086	0.6782	0.6504	0.6048	0.6054
Test Recall	0.7783	0.7121	0.7019	0.5305	0.4593	0.4141

Table 3: Comparison of Model Performances with ARWSADMM, FedAVG, and Local Training

Our experimental results, as summarized in Table 3, demonstrate the superior performance of our proposed AESADMM algorithm for Proximal Federated Learning. For the ResNet-50 model, AESADMM outperforms both FedAVG and Local training across all key performance indicators. With an F1 score of 79.33%, AESADMM shows enhanced prediction reliability, being 6.27% more accurate than FedAVG and 7.16 % than Local training. AESADMM also leads in precision (75.41%) and recall (77.83%), reflecting its robustness in handling diverse datasets and its capacity to minimize error in all class predictions and retrievals. When deployed on the EffNet-B0 architecture, the variant ARWSADMM continues to showcase enhanced performance. ARWSADMM records a training accuracy of 54.84%, The F1 score improvement is pronounced, with ARWSADMM scoring 49.42%, exceeding FedAVG by 10.01% and Local by 10.41%. This robust performance attests to the potential of our proposed method in addressing BMI prediction challenges, thereby providing a compelling solution for real-world applications requiring decentralized health data processing.

5 Conclusion

In this study, we introduced a novel Proximal Federated Learning (PFL) approach, proposing a novel and efficient algorithm called Adaptive Elastic Stochastic Alternating Direction Method of Multipliers (AESADMM) for training BMI federated classification model using commodity WiFi devices. Our method utilizes Channel State Information (CSI) to provide a privacy-preserving, non-intrusive BMI monitoring solution, eliminating active participant involvement. Empirical evaluations show that our approach outperforms traditional federated learning in privacy, accuracy, and efficiency. This research paves the way for scalable, cost-effective health monitoring solutions, potentially enhancing proactive health management and preventive care strategies.

References

[1] Peter Anthamatten, Deborah SK Thomas, Devon Williford, Jennifer C Barrow, Kirk A Bol, Arthur J Davidson, Sara J Deakyne Davies, Emily McCormick Kraus, David C Tabano, and Matthew F Daley. 2020. Geospatial monitoring of body mass index: use of electronic health record data across health care systems. *Public Health Reports* 135, 2 (2020), 211–219.

[2] Jianyang Ding, Yong Wang, and Xiangcong Fu. 2020. Wihi: WiFi based human identity identification using deep learning. *IEEE Access* 8 (2020).

[3] Jason S Fish, Susan Ettner, Alfonso Ang, and Arleen F Brown. 2010. Association of perceived neighborhood safety on body mass index. *American journal of public health* 100, 11 (2010), 2296–2303.

[4] Glenn Forbes. 2021. CSIKit: Python CSI processing and visualisation tools for commercial off-the-shelf hardware. https://github.com/Gi-z/CSIKit

[5] Valerio Frascolla, Dave Cavalcanti, and Rahul Shah. 2022. Wi-Fi Evolution: The Path Towards Wi-Fi 7 and Its Impact on IIoT. *Journal of Mobile Multimedia* 19, 01 (Sep. 2022), 263–276. https://doi.org/10.13052/jmm1550-4646.19113

[6] Sami Gabriel, RW Lau, and Camelia Gabriel. 1996. The dielectric properties of biological tissues: II. Measurements in the frequency range 10 Hz to 20 GHz. *Physics in medicine & biology* 41, 11 (1996), 2251.

[7] Joshua C Gonzales, Joshua Ron G Garcia, and Jocelyn F Villaverde. 2022. BMI Estimation from 2D Face Images Using Support Vector Machine. In *2022 6th International Conference on Communication and Information Systems (ICCIS)*. IEEE, 118–123.

[8] Zhi Jin, Junjia Huang, Wenjin Wang, Aolin Xiong, and Xiaojun Tan. 2022. Estimating human weight from a single image. *IEEE Transactions on Multimedia* (2022).

[9] J Sathish Kumar and Dhiren R Patel. 2014. A survey on internet of things: Security and privacy issues. *International Journal of Computer Applications* 90, 11 (2014).

[10] Qinbin Li, Bingsheng He, and Dawn Song. 2021. Model-contrastive federated learning. In *Proceedings of the IEEE/CVF conference on computer vision and pattern recognition*. 10713–10722.

[11] Tian Li, Shengyuan Hu, Ahmad Beirami, and Virginia Smith. 2021. Ditto: Fair and robust federated learning through personalization. In *International conference on machine learning*. PMLR, 6357–6368.

[12] Yongsen Ma, Gang Zhou, and Shuangquan Wang. 2019. WiFi sensing with channel state information: A survey. *ACM Computing Surveys (CSUR)* 52, 3 (2019), 1–36.

[13] Taishin Mabuchi, Yoshiaki Taniguchi, and Kimiaki Shirahama. 2020. Person recognition using Wi-Fi channel state information in an indoor environment. In *2020 IEEE International Conference on Consumer Electronics-Taiwan (ICCE-Taiwan)*. IEEE, 1–2.

[14] Brendan McMahan, Eider Moore, Daniel Ramage, Seth Hampson, and Blaise Aguera y Arcas. 2017. Communication-efficient learning of deep networks from decentralized data. In *Artificial intelligence and statistics*. PMLR, 1273–1282.

[15] Parisa Fard Moshiri, Hojjat Navidan, Reza Shahbazian, Seyed Ali Ghorashi, and David Windridge. 2020. Using GAN to enhance the accuracy of indoor human activity recognition. *arXiv preprint arXiv:2004.11228* (2020).

[16] Gabriela Nasser. 2020. Fighting childhood obesity in Brazil: a grassroots perspective. *European Journal of Public Health* 30, Supplement_5 (2020), ckaa166–474.

[17] Ziba Parsons, Fei Dou, Houyi Du, Zheng Song, and Jin Lu. 2024. Mobilizing personalized federated learning in infrastructure-less and heterogeneous environments via random walk stochastic ADMM. *Advances in Neural Information Processing Systems* 36 (2024).

[18] Wanbin Qi, Ronghui Zhang, Jiaen Zhou, Hao Zhang, Yanxi Xie, and Xiaojun Jing. 2023. A Resource-Efficient Cross-Domain Sensing Method for Device-Free Gesture Recognition With Federated Transfer Learning. *IEEE Transactions on Green Communications and Networking* 7, 1 (2023), 393–400. https://doi.org/10.1109/TGCN.2022.3233825

[19] Kun Qian, Chenshu Wu, Zimu Zhou, Yue Zheng, Zheng Yang, and Yunhao Liu. 2017. Inferring motion direction using commodity wi-fi for interactive exergames. In *Proceedings of the 2017 CHI conference on human factors in computing systems*. 1961–1972.

[20] Ronald W. Schafer. 2011. What Is a Savitzky-Golay Filter? [Lecture Notes]. *IEEE Signal Processing Magazine* 28, 4 (2011), 111–117. https://doi.org/10.1109/MSP.2011.941097

[21] Canh T Dinh, Nguyen Tran, and Josh Nguyen. 2020. Personalized federated learning with moreau envelopes. *Advances in neural information processing systems* 33 (2020), 21394–21405.

[22] Alysa Ziying Tan, Han Yu, Lizhen Cui, and Qiang Yang. 2022. Towards personalized federated learning. *IEEE transactions on neural networks and learning systems* 34, 12 (2022), 9587–9603.

[23] Fei Wang, Sanping Zhou, Stanislav Panev, Jinsong Han, and Dong Huang. 2019. Person-in-WiFi: Fine-grained person perception using WiFi. In *Proceedings of the IEEE/CVF International Conference on Computer Vision*. 5452–5461.

[24] Xuyu Wang, Chao Yang, and Shiwen Mao. 2017. TensorBeat: Tensor decomposition for monitoring multiperson breathing beats with commodity WiFi. *ACM Transactions on Intelligent Systems and Technology (TIST)* 9, 1 (2017), 1–27.

[25] Sharon B Wyatt, Karen P Winters, and Patricia M Dubbert. 2006. Overweight and obesity: prevalence, consequences, and causes of a growing public health problem. *The American journal of the medical sciences* 331, 4 (2006), 166–174.

[26] Tong Xin, Bin Guo, Zhu Wang, Pei Wang, Jacqueline Chi Kei Lam, Victor Li, and Zhiwen Yu. 2018. FreeSense: A robust approach for indoor human detection using Wi-Fi signals. *Proceedings of the ACM on Interactive, Mobile, Wearable and Ubiquitous Technologies* 2, 3 (2018), 1–23.

[27] Siamak Yousefi, Hirokazu Narui, Sankalp Dayal, Stefano Ermon, and Shahrokh Valaee. 2017. A survey on behavior recognition using WiFi channel state information. *IEEE Communications Magazine* 55, 10 (2017), 98–104.

[28] Jin Zhang, Fuxiang Wu, Bo Wei, Qieshi Zhang, Hui Huang, Syed W Shah, and Jun Cheng. 2020. Data augmentation and dense-LSTM for human activity recognition using WiFi signal. *IoTJ* 8, 6 (2020), 4628–4641.

[29] Xiaolong Zheng, Jiliang Wang, Longfei Shangguan, Zimu Zhou, and Yunhao Liu. 2016. Smokey: Ubiquitous smoking detection with commercial WiFi infrastructures. In *IEEE INFOCOM 2016-The 35th Annual IEEE International Conference on Computer Communications*. IEEE, 1–9.

[30] Ningjie Zhou, Weize Sun, and Mingjiong Liang. 2020. Human Activity Recognition based on WiFi Signal Using Deep Neural Network. In *International Conference on Smart City and Informatization (iSCI)*. IEEE, 26–30.